Published in final edited form as:

Leukemia. 2015 April ; 29(4): 869–876. doi:10.1038/leu.2014.289.

Clonal Evolution Revealed by Whole Genome Sequencing in a Case of Primary Myelofibrosis Transformed to Secondary Acute Myeloid Leukemia

Elizabeth K. Engle[1,*], **Daniel A.C. Fisher**[1,*], **Christopher A. Miller**[2], **Michael D. McLellan**[2], **Robert S. Fulton**[2], **Deborah M. Moore**[1], **Richard K. Wilson**[2], **Timothy J. Ley**[3], and **Stephen T. Oh**[1]

[1]Division of Hematology, Washington University School of Medicine, St. Louis, MO

[2]The Genome Institute, Washington University School of Medicine, St. Louis, MO

[3]The Genome Institute, Division of Oncology, Washington University School of Medicine, St. Louis, MO

Abstract

Clonal architecture in myeloproliferative neoplasms (MPNs) is poorly understood. Here we report genomic analyses of a patient with primary myelofibrosis (PMF) transformed to secondary acute myeloid leukemia (sAML). Whole genome sequencing (WGS) was performed on PMF and sAML diagnosis samples, with skin included as a germline surrogate. Deep sequencing validation was performed on the WGS samples and an additional sample obtained during sAML remission/relapsed PMF. Clustering analysis of 649 validated somatic single nucleotide variants revealed four distinct clonal groups, each including putative driver mutations. The first group (including *JAK2* and *U2AF1*), representing the founding clone, included mutations with high frequency at all three disease stages. The second clonal group (including *MYB*) was present only in PMF, suggesting the presence of a clone that was dispensable for transformation. The third group (including *ASXL1*) contained mutations with low frequency in PMF and high frequency in subsequent samples, indicating evolution of the dominant clone with disease progression. The fourth clonal group (including *IDH1* and *RUNX1*) was acquired at sAML transformation and was predominantly absent at sAML remission/relapsed PMF. Taken together, these findings illustrate the complex clonal dynamics associated with disease evolution in MPNs and sAML.

Keywords

Myelofibrosis; secondary acute myeloid leukemia; clonal evolution

Corresponding author: Stephen Oh, M.D., Ph.D. Division of Hematology, Washington University School of Medicine, 660 S. Euclid Ave, Campus Box 8125, St. Louis, MO 63110, Phone: (314) 362-8846, Fax: (314) 362-8826, stoh@dom.wustl.edu.

*These authors contributed equally to this work.

Conflict of interest disclosure: The authors declare no competing financial interest.

Supplementary information is available on the Leukemia website

Introduction

Myeloproliferative neoplasms (MPNs) are clonal myeloid malignancies that are derived from hematopoietic stem/progenitor cells (HSPCs).(1) These chronic disorders are characterized by unrestrained cellular proliferation leading to overproduction of one or more myeloid lineages. Primary myelofibrosis (PMF) is a subtype of MPN characterized by megakaryocyte hyperplasia and atypia, bone marrow fibrosis, extramedullary hematopoiesis, and splenomegaly.(2) The overall prognosis for PMF is poor, with expected survival ranging from months to several years.(3) In addition, patients with PMF exhibit a propensity for transformation to secondary acute myeloid leukemia (sAML), for which the prognosis is dismal.(4, 5)

The genetic basis of MPNs has been an area of intense investigation, notably marked by the identification of the *JAK2* V617F mutation.(6-9) Approximately 50-60% of patients with PMF harbor the *JAK2* V617F mutation, and an additional subset of patients (∼5-10%) exhibit mutations in other members of the JAK-STAT signaling axis such as *MPL*(10, 11) or *LNK (SH2B3)*.(12, 13) These findings indicate that dysregulated JAK-STAT signaling is a hallmark of MPN pathogenesis. In support of this notion, both *JAK2* V617F-positive and *JAK2* V617F-negative MF patients have exhibited clinical responses to treatment with targeted inhibitors of JAK2.(14, 15)

Despite these findings, recent studies have demonstrated that *JAK2* (or *MPL* or *LNK*) mutations are not the sole genetic lesion in many MPN cases.(16) *TET2* mutations may be acquired prior to the *JAK2* V617F mutation, indicating that at least in some MPNs there is a "pre-*JAK2*" event leading to clonal hematopoiesis.(17) This notion is supported by recent exome sequencing studies in which a subset of MPN patients were found to harbor pre-*JAK2* mutations.(18) Alterations in several genes (e.g. *IKZF1*, *p53*) are specifically associated with transformation to sAML.(16) Interestingly, sAML arising from a *JAK2* V617F-positive MPN frequently lacks the *JAK2* V617F mutation, suggesting that the leukemic clone in these cases originated from a pre-*JAK2* clone.(19) Recurrent mutations in several other genes (e.g. *ASXL1*, *EZH2*, *DNTM3A*, *IDH1/2*, *CBL*, *SRSF2*, *CALR*) have also recently been identified in MPNs.(20-22) Many of these mutations have been identified in chronic as well as blast phase MPNs. The specific role of these genes in disease initiation and/or progression remains incompletely understood.

Clonal hierarchy in MPNs, particularly in the context of disease progression, is not well defined. While exome sequencing studies can suggest possible clonal populations,(18, 22) this approach lacks the resolution to confidently define subclonal populations, primarily due to the low number of coding mutations typically found in myeloid malignancies.(23, 24) In addition, small subclonal populations may only be detected when multiple timepoints are assessed. Previous studies investigating clonal evolution in MPNs have primarily focused on selected gene mutations or chromosome 9p UPD encompassing *JAK2*.(25-28) The only whole genome sequencing (WGS) study in MPNs published to date examined a single patient with early stage PMF and did not examine multiple timepoints or disease evolution.(29)

Here we report comprehensive genomic analyses performed on an individual patient with PMF transformed to sAML. WGS in conjunction with deep sequencing validation enabled clonal modeling of multiple disease stages, thereby inferring mechanisms of disease evolution.

Materials and Methods

Patient samples

Bone marrow, peripheral blood, and skin samples were obtained from a single patient at three different disease stages (PMF, sAML, sAML remission/relapsed PMF). Genomic DNA was extracted from PMF and sAML bone marrow mononuclear cells, as well as from peripheral blood mononuclear cells obtained during sAML remission/relapsed PMF. Genomic DNA was extracted from a skin biopsy collected at PMF diagnosis. The patient provided written consent on a protocol approved by the Washington University Human Studies Committee (WU #01-1014) that includes specific language authorizing WGS.

Whole genome sequencing and variant detection

WGS was performed on the PMF, sAML, and skin (normal) samples. For WGS, paired-end sequencing was performed using the Illumina HiSeq platform with 100 bp read length (San Diego, CA). For the PMF and sAML samples, 211.9 to 212.9Gb of WGS sequence was generated (corresponding to 63.9x and 60.2x haploid coverage of the reference genome, respectively), and for the normal sample 127.1Gb was generated (corresponding to 37.5x haploid coverage). Alignment of reads and detection of somatic mutations (single nucleotide, indel, and structural variants) was performed as described previously(24), with updates to the versions of the following tools: BWA v0.5.9(30), Picard v1.46 (http://picard.sourceforge.net/), dbSNP build 132(31), Samtools svn rev 963(32), and Pindel v0.5.(33) Single nucleotide variants (SNVs) and indels were binned into tiers as previously described (34), where tier 1 includes mutations in the coding regions of exons, consensus splice sites, and RNA genes, tier 2 includes mutations in highly conserved genomic regions and regions with regulatory potential, tier 3 includes mutations in the nonrepetitive portion of the genome not included in tier 2, and tier 4 mutations are in the remainder of the genome.

Somatic copy number alterations were detected using copyCat version 1.5 (https://github.com/chrisamiller/copycat). Possible regions of copy number alteration were investigated by plotting the ratio of tumor to reference WGS reads normalized to the average tumor: reference ratio across the chromosome for all SNVs in the candidate region. Copy number neutral loss of heterozygosity was detected on chromosome 9 from bases 1 to 8783029 in both the PMF and sAML samples using SNP calls from Varscan and segmented with the DNAcopy package for R.(35)

RNA sequencing and analysis

RNA sequencing was performed on the PMF and sAML samples. Paired-end sequencing was performed on poly-A selected RNA using the Illumina HiSeq2000 platform with 100 bp read length. For the PMF and sAML samples, 397 and 393 million total reads were

generated, respectively. Reads were aligned with TopHat v1.3.1 (36) and analyzed with Cufflinks v1.0.3.(37) The resulting transcript abundance estimates are expressed in fragments per kilobase of exon per million fragments mapped (FPKM), as proposed by Mortazavi et al.(38) Gene fusions were detected from RNA sequencing data using BreakFusion version 1.0.(39)

Validation sequencing and variant detection

A capture panel was designed for validation resequencing. A customized capture array design targeting 10,307,042 bases was made by Roche NimbleGen (Madison, WI), and libraries were hybridized according to the manufacturer's protocol. The array included all tier 1-3 high confidence SNVs (1,351), tier 1 low confidence SNVs (48,884), tier 1-3 indels (5,549) and structural variants (22,442) identified in the WGS. In addition, capture probes targeting SNVs and exons in genes known or predicted to be associated with MPN pathogenesis (Supplementary Table 1) were obtained from Integrated DNA Technologies (Coralville, IA). These additional probes targeting 80,880 bases were spiked into the Roche Nimblegen (Madison, WI) capture panel at a 2:1 ratio.

Validation sequencing was performed on the three WGS samples as well as a fourth sample obtained during sAML remission/relapsed PMF. Sequence was produced on the Illumina HiSeq2000 platform and runs were completed according to the manufacturer's recommendations (Illumina Inc, San Diego, CA). Between 2.7 and 4.9 Gb of sequence was produced for each sample, giving a median target coverage of 216x to 388x. Variants were detected using Somatic Sniper v0.7.3 (40), GATK (41), Pindel v0.5, and Varscan v2.2.6 (42), then validated as described previously.(24) All validated SNVs had a VAF of at least 11% in the sample in which it was validated. In order to follow the frequency of a SNV or indel across disease progression, if a mutation was validated in at least one sample, the frequency of that mutation in other samples was retained regardless of individual sample validation results. In some instances this led to the retention of mutations with extremely low VAFs. In these cases it could not be completely excluded that the low VAFs were in fact due to base calling errors.

Clustering

Validated SNVs in the PMF and sAML samples enabled the identification of clonal groups using a clustering strategy similar to Walter et al.(43) The variant allele frequencies (VAFs) of three SNVs in a region of uniparental disomy (UPD) on chromosome 9 (first 8.7 MB) were divided in half prior to clustering. Outlier VAFs were detected by dbscan (44), with a reachability index of 0.5. VAF data along with outlier points submitted as potential noise were submitted for unsupervised clustering using the Mclust algorithm (45) with default parameters. The maximum number of clusters was limited to four (G=1:4), and each cluster had to contain at least seven SNVs (1% of the total number of SNVs). Out of 10 available models in Mclust, an ellipsoidal model with variable volume and orientation but equal shape was selected as the best model and contained three groups.

Validated SNVs in the sAML remission/relapsed PMF sample refined the clusters. Initial unsupervised clustering of the PMF and sAML samples identified a single group with high

sAML VAFs and low PMF VAFs. Based on the VAFs in the sAML remission/relapsed PMF sample, the cluster was divided into two groups: “Low PMF” or “sAML only”. The SNVs in the “Low PMF” group had VAFs > 19% in the sAML remission/relapsed PMF sample. The “sAML only” SNVs were characterized by VAFs < 2.6% in the PMF stage and < 2% in the sAML remission/relapsed PMF sample. The result was four clusters of SNVs that corresponded to the founding clone and three subclones observed across the three samples.

Genotyping *JAK2* and *U2AF1* mutations in individual colonies

Peripheral blood from the PMF stage was stained with antibodies against CD34, CD38, CD3, CD19, CD14, and CD16. Lineage-negative CD34+ cells were sorted on a Dako MoFlo flow cytometer (Beckman-Coulter Inc, Indianapolis, IN) and plated at one cell per well into 96-well plates containing a monolayer of AFT024 mouse bone marrow stromal cells. After growth for 28-35 days in vitro, DNA from individual colonies was extracted using the QiaAmp DNA mini kit (Qiagen, Bergisch Gladbach, Germany). Colony DNA was genotyped for *JAK2* V617F and *U2AF1* Q157P mutations by TaqMan real time PCR on a StepOne Plus real time thermal cycler (Applied Biosystems/Life Technologies, Grand Island, NY). The *JAK2* V617F PCR was a modified version of the protocol by Levine et al. (46) The *U2AF1* Q157P TaqMan PCR assay utilized forward primer = CCGTGACGGACTTCAGAGAA, reverse primer = ACTGGCCACTCCTCACTCA, WT probe = VIC-CTGCCGTCAGTATGAG-MGB, and Q157P probe = 6FAM-TGCCGTCCGTATGAG-MGB, with an annealing temperature of 60°C. Genotyping was calibrated with HEL cell line DNA (*JAK2* V617F homozygous) mixed in a titration series with control *JAK2* wild-type human genomic DNA, and whole bone marrow DNA from the PMF stage. Genotyping for each colony was considered successful if consistent genotype results were obtained for both *JAK2* and *U2AF1* PCRs. Of 202 CD34+ cell derived colony DNAs genotyped, 42 had consistent genotype results for both the *JAK2* V617F and *U2AF1* Q157P mutations.

Results

Case history

A 51 year-old woman initially presented with splenomegaly, pancytopenia, and leukoerythroblastosis (Supplementary Table S2). A bone marrow biopsy demonstrated severe fibrosis, consistent with a diagnosis of PMF. Cytogenetics were normal. Bone marrow and skin samples were banked at that time. The patient had an excellent response to treatment with thalidomide, ultimately achieving a complete hematologic remission. Due to the development of neuropathy, therapy was eventually switched to lenalidomide. Seven years after initial PMF diagnosis, the patient transformed to sAML. A bone marrow biopsy revealed 49% blasts, and cytogenetics were normal. Testing for *JAK2* V617F was positive. Bone marrow samples were again banked. The patient received induction chemotherapy with IDA-FLAG (idarubicin, fludarabine, cytarabine, G-CSF) and attained a complete remission, followed by consolidation chemotherapy with four cycles of high-dose cytarabine. Subsequently, the patient declined bone marrow transplantation. Approximately 1.5 years after sAML diagnosis, the patient again developed pancytopenia with

leukoerythroblastosis, consistent with relapsed PMF, but with no evidence of sAML relapse. Peripheral blood samples were banked approximately two years after sAML diagnosis. Samples were thus banked at three stages: PMF diagnosis, sAML diagnosis, and sAML remission/relapsed PMF.

Whole genome sequencing and capture validation

WGS was performed on the PMF and sAML patient samples, as well as a skin sample obtained at PMF diagnosis. The latter served as a normal control to exclude potential germline variants. Haploid coverage was 64x, 60x, and 38x for the PMF, sAML, and skin samples, respectively. Potential somatic mutations were identified and divided into four tiers as previously described.(34) Tier 1 mutations included mutations in protein coding sequences, consensus splice sites and RNA genes. Somatic single nucleotide mutations (SNVs) and insertions and deletions (indels) were validated using custom capture to enable deep sequencing of each mutation. A fourth sample, the sAML remission/relapsed PMF sample, was included in the validation analysis, thereby adding a third timepoint to compare mutation frequencies over time with disease progression.

A total of 649 SNVs were validated in at least one of the three tumor samples (Table 1, Supplementary Table S3 and S4). Of the 649 SNVs, all had over 100x coverage with the exception of three SNVs with just under 100 reads in the sAML sample. An average of 398, 302, and 537 reads spanned the validated mutations in the PMF, sAML, and sAML remission/relapsed PMF samples, respectively. In addition, two tier 1 indels were validated, along with 127 tier 2 and 3 indels (Supplementary Table S3 and S4) No structural variants (Supplementary Table S5) or gene fusions (Supplementary Table S6) were identified that likely contributed to disease progression due to the absence of either in the sAML sample.

Seven years passed between the collection of the PMF sample and the sAML sample, and a corresponding increase in the total number of SNVs from 440 to 562 was observed (Table 1). The proportion of SNVs in tiers 1-3 was similar between the PMF and sAML samples and for the SNVs that were gained between PMF and sAML, suggesting that the majority of SNVs were randomly distributed across the genome. There was no overrepresentation of tier 1 SNVs gained in the sAML sample, indicating that disease progression was not accompanied by a specific increase in coding mutations. The observed number of coding SNVs per sample fell within the calculated range of coding mutations expected to accumulate in HSPCs each year as a result of errors during DNA replication,(23) suggesting that the majority of the mutations were due to the aging process. This was also consistent with genome-wide studies in MDS and AML which concluded that the majority of somatic SNVs are passenger mutations that accumulate over time (23, 34, 43).

An increased proportion of transversion mutations may be indicative of therapy-related DNA changes.(23, 47) For the PMF and sAML samples, the transition and transversion frequencies were roughly similar to previously published studies of AML, MDS, and MPNs (Figure 1).(22, 23, 43) sAML-specific mutations from the patient examined in this study also had a similar distribution. These findings indicate that there was no obvious therapy-related effect on mutation distribution in this case.

Putative MPN and sAML driver mutations

A total of 38 tier 1 SNVs were validated across the three tumor samples (Figure 2, Supplementary Table 3). Of the validated tier 1 SNVs, six were identified as putative driver mutations (*JAK2*, *U2AF1*, *MYB*, *ASXL1*, *RUNX1*, *IDH1*) based on prior studies demonstrating mutations in each of these genes in MPNs and/or sAML (Table 2).(20, 48-51) The *JAK2* and *U2AF1* mutations were identified in all three samples with a variant allele frequency (VAF) of approximately 75% and 40%, respectively. The *MYB* mutation was present in the PMF sample at a VAF of 20%, but was not detectable in the sAML or sAML remission/relapsed PMF samples. A mutation in *ASXL1* was found at a low frequency (6%) in the PMF sample, but was substantially enriched in the sAML (44%) and sAML remission/relapsed PMF (32%) samples. *RUNX1* and *IDH1* mutations were validated only in the sAML sample at VAFs of 35 and 30%, respectively. Amongst the remaining 32 tier 1 SNVs, a mutation in the *HCFC1* gene was identified as an additional possible driver based on its expression, known function and interaction in pathways also involving *ASXL1*.(52-54) This mutation followed a VAF pattern across the three different disease stages that was quite similar to *ASXL1*, suggesting a possible synergy between the two mutations.

RNA sequencing data confirmed that all candidate driver mutations (Table 2) were expressed in the corresponding PMF and/or sAML samples (Supplementary Table 3). Out of the 40 tier 1 mutations inclusive of SNVs and indels, 18 were expressed in the PMF and/or sAML samples. Most mutations had a similar VAF in the validated whole genome sequencing data compared to the RNA sequencing data (Supplementary Figure 1).

JAK2 V617F homozygosity is an early event

The *JAK2* V617F mutation may initially be acquired as a heterozygous mutation and subsequently become homozygous via mitotic recombination (27, 55, 56). To establish whether the VAF observed for the *JAK2* V617F mutation corresponded primarily to a dominant *JAK2* V617F homozygous clone, or to a mixture of *JAK2* V617F homozygous and heterozygous clonal populations, colonies derived from individual CD34+ cells from the PMF stage were grown *in vitro* to identify the predominant genotypes among individual clones. Genotyping by real-time PCR verified that the observed CD34+-derived cell population was predominantly *JAK2* V617F homozygous, with 69% of colonies homozygous, less than 5% heterozygous for *JAK2* V617F, and 26% *JAK2* homozygous wild-type (Table 3). Based on these results, the imputed *JAK2* V617F allele frequency in the genotyped colonies was 71.4%. This was similar to the 71.2% from bulk sorted CD34+ cells, suggesting that culturing the CD34+ cells did not significantly alter the *JAK2* V617F VAF. Both VAFs were similar to the 74.4% observed by deep sequencing of the bone marrow from the PMF stage. Thus, the single cell-derived clones observed *in vitro* appeared to be representative of those *in vivo*, implying that the *in vivo* cell population was predominantly *JAK2* V617F homozygous. By the overt establishment of PMF, the homozygous mutant cell population was already dominant over the heterozygous population.

Since the *JAK2* and *U2AF1* mutations were the most abundant candidate driver mutations identified at the PMF stage, either could represent the founding mutation of the PMF

propagating clone. To establish which mutation may have arisen first, colony DNAs were also genotyped for the *U2AF1* Q157P mutation. As shown in Table 3, the *U2AF1* mutation was present only in cells also containing *JAK2* V617F. The predominant *JAK2* V617F homozygous cell population was almost entirely *U2AF1* Q157P heterozygous, consistent with an observed VAF for *U2AF1* Q157P roughly half of that observed for *JAK2* V617F. There were too few *JAK2* heterozygous cells observed to determine definitively which mutation, *JAK2* or *U2AF1*, preceded the other. It can only be concluded that by the onset of PMF, a *JAK2* V617F homozygous, *U2AF1* Q157P heterozygous clone had outcompeted all previous mutant clonal populations.

Clonal architecture

With over four hundred SNVs per sample, the clonal architecture during disease progression could be inferred. The VAFs of copy neutral mutations were clustered to identify the predominant clone and subclonal populations accompanying disease evolution. Since there was no evidence for copy number variation around any of the validated SNVs, all validated SNVs were considered copy number neutral and were included in modeling clonality.

The *JAK2* V617F mutation and two additional SNVs were located in a region of uniparental disomy (UPD) in the first 8.78 Mb of chromosome 9 and had apparent copy number neutral loss of heterozygosity. Consistent with the observation of UPD, all three SNVs had VAFs of approximately 75% across samples, and genotyping indicated that the majority of cells were homozygous for the *JAK2* V617F mutation. As a result, the VAFs for each of the three mutations (including *JAK2* V617F) were divided in half for clonal modeling, resulting in VAFs of approximately 37%.

Using the assumption that mutations with similar VAFs represented a clonal group and traveled together, clonal groups were identified based on clusters of VAFs. Unsupervised clustering of the VAFs from the PMF and sAML sample identified a founding clone and two subclones (Figure 3A). The frequency of variants in the sAML remission/relapsed PMF sample provided a third timepoint to resolve clonal groups and showed that there was a founding clone and three subclones (Figure 3B). The sAML remission/relapsed PMF sample distinguished between a sAML-only clonal group and a clonal group that had a high VAF at both sAML and sAML remission/relapsed PMF. Based on the clustering results, a model of clonal progression was developed demonstrating the dynamics of clonal evolution across disease progression (Figure 3C).

Discussion

This study delineates clonal evolution in a patient who initially presented with PMF, transformed to sAML, and subsequently experienced prolonged sAML remission despite PMF relapse. Bone marrow genomic DNA was cytogenetically normal at both PMF and sAML stages, and no large structural variant or gene fusion contributing to disease progression was detected. Therefore, the total somatic mutational burden identified at the PMF and sAML stages could be attributed to a combination of SNVs and small indels. Seven candidate driver SNVs were identified in the PMF and/or sAML samples. These

candidate driver mutations corresponded to the founding clone and subsequent subclones identified in the PMF and sAML disease stages.

The overall burden of acquired mutations in this patient was similar to those previously reported for *de novo* AML and normal aging of the hematopoietic system.(23) The transversion frequency and the ratio of tier 1:2:3 mutations was consistent with healthy aging(23) as well as previous observations in *de novo* AML(23), myelodysplastic syndromes (MDS), and post-MDS sAML(43). With respect to MPNs, a single published WGS study describing a patient with PMF at chronic phase(29) and recently published exome sequencing studies(21, 22, 57) have not suggested a substantially different mutational burden in MPNs from what has been observed in this study or in normal aging. Taken together, these observations indicate that the majority of somatic mutations in this patient were most likely passenger mutations acquired in the context of normal aging of the HSPC population.

A total of 40 tier 1 SNVs and indels were identified via WGS and validated by custom capture sequencing. The majority of these were categorized as likely passenger mutations based on absence of expression by RNA sequencing, codon synonymity, and/or predicted benign alteration in a protein (Supplementary table 3). However, it could not be definitively excluded that a subset of these mutations may have pathogenetic relevance. Six genes (*JAK2*, *U2AF1*, *MYB*, *ASXL1*, *IDH1*, and *RUNX1*) were identified as likely candidate driver mutations, largely based on known recurrence of mutations in these genes in MPNs and/or sAML.(20, 48-51) A seventh gene (*HCFC1*) was identified as a possible driver mutation based on its known functions and interaction with *ASXL1*.(52-54)

The PMF stage was characterized by a founding clone harboring mutations in *JAK2* and *U2AF1*, a large subclone containing a mutation in *MYB*, and a minor subclone containing mutations in *ASXL1* and *HCFC1*. The SNVs in *JAK2* and *U2AF1* were representative of a dominant clone at all disease stages. The high VAF of *JAK2* V617F suggested prevalent homozygosity at all stages. Single colony genotyping confirmed that the CD34+ cell population was predominantly *JAK2* V617F homozygous at the PMF stage, with the residual population being wild-type for *JAK2*, and *JAK2* V617F heterozygous clones being rare.

Based on single colony genotyping, it could not be resolved which of the mutations in *JAK2* and *U2AF1* preceded the other in the evolution of the malignant clone. Given the dominance of the clone containing these mutations at the PMF stage, both mutations were likely early events. Based on the stage-specific clonality or subclonality of the candidate driver mutations, the PMF dominant clone was driven predominantly if not exclusively by the *JAK2* and *U2AF1* mutations, with the *MYB* mutation being a likely subclonal driver, albeit one that was extinct by the time of sAML diagnosis. Since the *MYB* mutation was not identified in the relapsed MF, these observations suggest that the combination of *JAK2* V617F homozygosity and *U2AF1* Q157P heterozygosity was sufficient to initiate PMF in this patient.

ASXL1 and *HCFC1* mutations were present in a small subclone at the PMF stage that expanded with transformation and remained at high frequency at sAML remission/relapsed

PMF. The combination of mutations in *ASXL1* and *HCFC1* was particularly notable because their protein products are known bind to each other and are present together in complexes with several other known oncogenes and tumor suppressors with diverse biological roles including regulation of histone methylation.(52-54) In a mouse model, absence of one such shared binding partner, BAP1, led to a lack of HCFC1 protein (since BAP1 normally prevents HCFC1 degradation), and these mice exhibited features of myeloproliferative disease.(52) Although recurrent *HCFC1* mutations have not been identified thus far in large-scale exome sequencing studies in MPNs,(18, 21, 22) a mutation in *HCFC1* was found in one case of *de novo* AML.(24). Collectively, these findings support the notion that *HCFC1* mutations may be pathogenic, and that *ASXL1* and *HCFC1* mutations could plausibly interact to contribute to disease evolution. However, the possibility that the *HCFC1* mutation in this case was a passenger mutation that randomly coincided with the mutation in *ASXL1* cannot be excluded.

The clone containing *ASXL1* and *HCFC1* mutations proliferated at the expense of the *MYB* mutant clone, and was parental to the sAML clone harboring *RUNX1* and *IDH1* mutations. The persistence of the *ASXL1* and *HCFC1* mutations at sAML remission/relapsed PMF suggests that the addition of these mutations to the *JAK2/U2AF1* mutant founding clone was not sufficient to induce transformation to sAML, which was likely precipitated by mutations in *RUNX1* and *IDH1*. The *ASXL1/HCFC1* mutant clone, however, was likely dominant over the parental *JAK2/U2AF1* mutant clone lacking these later mutations.

The sAML stage was characterized by the founding clone and two nested subclones, with one clone harboring *ASXL1 and HCFC1* mutations and the sAML-specific subclone additionally containing mutations in *RUNX1* and *IDH1*. The near total absence in the sAML remission/relapsed PMF sample of the *IDH1* and *RUNX1* mutations indicates that treatment predominantly eradicated the sAML specific subclone. However, the *RUNX1* mutation was identified at a very low frequency (0.7%) in the sAML remission/relapsed PMF sample, suggesting the presence of minimal residual disease and a potential for sAML relapse. Approximately one year following sAML remission, the patient did experience clinical sAML relapse. Biological samples were not available from the relapsed sAML stage to confirm that the *RUNX1* mutation was present, as would be predicted.

The availability of matched serial samples provided additional resolution regarding subclonal populations present at the PMF disease stage. Based only on the PMF validation data, there appeared to be a founding clone driven by mutations in *JAK2* and *U2AF1* and a subclone characterized by a mutation in *MYB*. However, by including the sAML data it became clear that while the *ASXL1* mutation was only present at low frequency in the PMF stage, it represented an additional subclone that expanded and likely contributed to leukemic transformation. As *ASXL1* is considered to be a high-risk mutation, its presence, even in a rare subclone, in the PMF stage is relevant to the biology of the patient's disease course.

To our knowledge, this represents the first study to analyze the progression from a chronic phase MPN to sAML by WGS and utilize deep sequencing validation to model clonal evolution across the disease stages. Future studies with this approach are needed to

determine whether consistent patterns of clonal evolution that drive MPN disease progression can be identified.

Supplementary Material

Refer to Web version on PubMed Central for supplementary material.

Acknowledgments

This work was supported by NIH grants K08HL106576 (Oh), K12HL087107 (Oh), P01CA101937 (Ley), and T32HL007088 (Engle, Fisher). This research was also supported by a Sidney Kimmel Scholar Award (Oh), Leukemia Research Foundation New Investigator Award (Oh), Central Society for Clinical Research Early Career Development Award (Oh), Barnes-Jewish Hospital Foundation/Washington University Institute of Clinical and Translational Sciences Pilot Grant (Oh), and American Cancer Society Institutional Research Grant (Oh). This work was supported by the Washington University Institute of Clinical and Translational Sciences grant UL1TR000448 from the National Center for Advancing Translational Sciences of NIH. Technical support was provided by the Alvin J. Siteman Cancer Center Tissue Procurement and Flow Cytometry Cores, which are supported by NCI Cancer Center Support Grant P30CA91842. The authors thank D. Link and J. Xia for assistance with cell sorting and colony assays, K. Martin, C. Kaiwar, and M. Fulbright for performing *JAK2* and *U2AF1* genotyping experiments, and J. McMichael for assistance with illustrations.

References

1. Levine RL, Gilliland DG. Myeloproliferative disorders. Blood. 2008 Sep 15; 112(6):2190–8. [PubMed: 18779404]
2. Tefferi A, Vainchenker W. Myeloproliferative neoplasms: molecular pathophysiology, essential clinical understanding, and treatment strategies. J Clin Oncol. 2011 Feb 10; 29(5):573–82. Epub 2011/01/12. eng. [PubMed: 21220604]
3. Gangat N, Caramazza D, Vaidya R, George G, Begna K, Schwager S, et al. DIPSS plus: a refined Dynamic International Prognostic Scoring System for primary myelofibrosis that incorporates prognostic information from karyotype, platelet count, and transfusion status. J Clin Oncol. 2011 Feb 1; 29(4):392–7. [PubMed: 21149668]
4. Heaney ML, Soriano G. Acute myeloid leukemia following a myeloproliferative neoplasm: clinical characteristics, genetic features and effects of therapy. Curr Hematol Malig Rep. 2013 Jun; 8(2): 116–22. [PubMed: 23572311]
5. Mesa RA, Li CY, Ketterling RP, Schroeder GS, Knudson RA, Tefferi A. Leukemic transformation in myelofibrosis with myeloid metaplasia: a single-institution experience with 91 cases. Blood. 2005 Feb 1; 105(3):973–7. [PubMed: 15388582]
6. Baxter EJ, Scott LM, Campbell PJ, East C, Fourouclas N, Swanton S, et al. Acquired mutation of the tyrosine kinase JAK2 in human myeloproliferative disorders. Lancet. 2005 Jan 1; 365(9464): 1054–61. eng. [PubMed: 15781101]
7. James C, Ugo V, Le Couedic JP, Staerk J, Delhommeau F, Lacout C, et al. A unique clonal JAK2 mutation leading to constitutive signalling causes polycythaemia vera. Nature. 2005 Apr 28; 434(7037):1144–8. Epub 2005/03/29. eng. [PubMed: 15793561]
8. Kralovics R, Passamonti F, Buser AS, Teo SS, Tiedt R, Passweg JR, et al. A gain-of-function mutation of JAK2 in myeloproliferative disorders. N Engl J Med. 2005 Apr 28; 352(17):1779–90. eng. [PubMed: 15858187]
9. Levine R, Wadleigh M, Cools J, Ebert B, Wernig G, Huntly BJ, et al. Activating mutation in the tyrosine kinase JAK2 in polycythemia vera, essential thrombocythemia, and myeloid metaplasia with myelofibrosis. Cancer Cell. 2005 Apr 1; 7(4):387–97. eng. [PubMed: 15837627]
10. Pardanani A, Levine R, Lasho T, Pikman Y, Mesa R, Wadleigh M, et al. MPL515 mutations in myeloproliferative and other myeloid disorders: a study of 1182 patients. Blood. 2006 Nov 15; 108(10):3472–6. [PubMed: 16868251]

11. Pikman Y, Lee BH, Mercher T, McDowell E, Ebert B, Gozo M, et al. MPLW515L is a novel somatic activating mutation in myelofibrosis with myeloid metaplasia. PLoS Med. 2006 Jul 1.3(7):e270. eng. [PubMed: 16834459]
12. Oh ST, Simonds EF, Jones C, Hale MB, Goltsev Y, Gibbs KD Jr, et al. Novel mutations in the inhibitory adaptor protein LNK drive JAK-STAT signaling in patients with myeloproliferative neoplasms. Blood. 2010 Aug 12; 116(6):988–92. Epub 2010/04/21. eng. [PubMed: 20404132]
13. Pardanani A, Lasho T, Finke C, Oh ST, Gotlib J, Tefferi A. LNK mutation studies in blast-phase myeloproliferative neoplasms, and in chronic-phase disease with TET2, IDH, JAK2 or MPL mutations. Leukemia. 2010 Oct; 24(10):1713–8. Epub 2010/08/21. eng. [PubMed: 20724988]
14. Verstovsek S, Mesa RA, Gotlib J, Levy RS, Gupta V, DiPersio JF, et al. A double-blind, placebo-controlled trial of ruxolitinib for myelofibrosis. N Engl J Med. 2012 Mar 1; 366(9):799–807. Epub 2012/03/02. eng. [PubMed: 22375971]
15. Harrison C, Kiladjian JJ, Al-Ali HK, Gisslinger H, Waltzman R, Stalbovskaya V, et al. JAK inhibition with ruxolitinib versus best available therapy for myelofibrosis. N Engl J Med. 2012 Mar 1; 366(9):787–98. Epub 2012/03/02. eng. [PubMed: 22375970]
16. Tefferi A. Mutations galore in myeloproliferative neoplasms: would the real Spartacus please stand up? Leukemia. 2011 Jul; 25(7):1059–63. Epub 2011/07/14. eng. [PubMed: 21750560]
17. Delhommeau F, Dupont S, Della Valle V, James C, Trannoy S, Masse A, et al. Mutation in TET2 in myeloid cancers. N Engl J Med. 2009 May 28; 360(22):2289–301. Epub 2009/05/29. eng. [PubMed: 19474426]
18. Wang L, Swierczek SI, Drummond J, Hickman K, Kim SJ, Walker K, et al. Whole-exome sequencing of polycythemia vera revealed novel driver genes and somatic mutation shared by T cells and granulocytes. Leukemia. 2014 Apr; 28(4):935–8. [PubMed: 24413320]
19. Theocharides A, Boissinot M, Girodon F, Garand R, Teo S, Lippert E, et al. Leukemic blasts in transformed JAK2-V617F-positive myeloproliferative disorders are frequently negative for the JAK2-V617F mutation. Blood. 2007 Jul 1; 110(1):375–9. [PubMed: 17363731]
20. Abdel-Wahab O. Genetics of the myeloproliferative neoplasms. Curr Opin Hematol. 2011 Feb 8. Epub 2011/02/11. Eng.
21. Klampfl T, Gisslinger H, Harutyunyan AS, Nivarthi H, Rumi E, Milosevic JD, et al. Somatic mutations of calreticulin in myeloproliferative neoplasms. N Engl J Med. 2013 Dec 19; 369(25): 2379–90. [PubMed: 24325356]
22. Nangalia J, Massie CE, Baxter EJ, Nice FL, Gundem G, Wedge DC, et al. Somatic CALR mutations in myeloproliferative neoplasms with nonmutated JAK2. N Engl J Med. 2013 Dec 19; 369(25):2391–405. [PubMed: 24325359]
23. Welch JS, Ley TJ, Link DC, Miller CA, Larson DE, Koboldt DC, et al. The origin and evolution of mutations in acute myeloid leukemia. Cell. 2012 Jul 20; 150(2):264–78. Epub 2012/07/24. eng. [PubMed: 22817890]
24. Cancer Genome Atlas Research N. Genomic and epigenomic landscapes of adult de novo acute myeloid leukemia. N Engl J Med. 2013 May 30; 368(22):2059–74. [PubMed: 23634996]
25. Wang L, Swierczek SI, Lanikova L, Kim SJ, Hickman K, Walker K, et al. The relationship of JAK2(V617F) and acquired UPD at chromosome 9p in polycythemia vera. Leukemia. 2014 Apr; 28(4):938–41. [PubMed: 24463469]
26. Wang X, LeBlanc A, Gruenstein S, Xu M, Mascarenhas J, Panzera B, et al. Clonal analyses define the relationships between chromosomal abnormalities and JAK2V617F in patients with Ph-negative myeloproliferative neoplasms. Exp Hematol. 2009 Oct; 37(10):1194–200. [PubMed: 19615425]
27. Godfrey AL, Chen E, Pagano F, Silber Y, Campbell PJ, Green AR. Clonal analyses reveal associations of JAK2V617F homozygosity with hematologic features, age and gender in polycythemia vera and essential thrombocythemia. Haematologica. 2013 May; 98(5):718–21. [PubMed: 23633544]
28. Lundberg P, Karow A, Nienhold R, Looser R, Hao-Shen H, Nissen I, et al. Clonal evolution and clinical correlates of somatic mutations in myeloproliferative neoplasms. Blood. 2014 Apr 3; 123(14):2220–8. [PubMed: 24478400]

29. Merker JD, Roskin KM, Ng D, Pan C, Fisk DG, King JJ, et al. Comprehensive whole-genome sequencing of an early-stage primary myelofibrosis patient defines low mutational burden and non-recurrent candidate genes. Haematologica. 2013 Nov; 98(11):1689–96. [PubMed: 23872309]
30. Li H, Durbin R. Fast and accurate short read alignment with Burrows-Wheeler transform. Bioinformatics. 2009 Jul 15; 25(14):1754–60. [PubMed: 19451168]
31. Sherry ST, Ward MH, Kholodov M, Baker J, Phan L, Smigielski EM, et al. dbSNP: the NCBI database of genetic variation. Nucleic Acids Res. 2001 Jan 1; 29(1):308–11. [PubMed: 11125122]
32. Li H, Handsaker B, Wysoker A, Fennell T, Ruan J, Homer N, et al. The Sequence Alignment/Map format and SAMtools. Bioinformatics. 2009 Aug 15; 25(16):2078–9. [PubMed: 19505943]
33. Ye K, Schulz MH, Long Q, Apweiler R, Ning Z. Pindel: a pattern growth approach to detect break points of large deletions and medium sized insertions from paired-end short reads. Bioinformatics. 2009 Nov 1; 25(21):2865–71. Epub 2009/06/30. eng. [PubMed: 19561018]
34. Mardis ER, Ding L, Dooling DJ, Larson DE, McLellan MD, Chen K, et al. Recurring mutations found by sequencing an acute myeloid leukemia genome. N Engl J Med. 2009 Sep 10; 361(11): 1058–66. Epub 2009/08/07. eng. [PubMed: 19657110]
35. Venkatraman ES, Olshen AB. A faster circular binary segmentation algorithm for the analysis of array CGH data. Bioinformatics. 2007 Mar 15; 23(6):657–63. [PubMed: 17234643]
36. Trapnell C, Pachter L, Salzberg SL. TopHat: discovering splice junctions with RNA-Seq. Bioinformatics. 2009 May 1; 25(9):1105–11. Epub 2009/03/18. eng. [PubMed: 19289445]
37. Trapnell C, Williams BA, Pertea G, Mortazavi A, Kwan G, van Baren MJ, et al. Transcript assembly and quantification by RNA-Seq reveals unannotated transcripts and isoform switching during cell differentiation. Nat Biotechnol. 2010 May; 28(5):511–5. Epub 2010/05/04. eng. [PubMed: 20436464]
38. Mortazavi A, Williams BA, McCue K, Schaeffer L, Wold B. Mapping and quantifying mammalian transcriptomes by RNA-Seq. Nat Methods. 2008 Jul; 5(7):621–8. Epub 2008/06/03. eng. [PubMed: 18516045]
39. Chen K, Wallis JW, Kandoth C, Kalicki-Veizer JM, Mungall KL, Mungall AJ, et al. BreakFusion: targeted assembly-based identification of gene fusions in whole transcriptome paired-end sequencing data. Bioinformatics. 2012 Jul 15; 28(14):1923–4. [PubMed: 22563071]
40. Larson DE, Harris CC, Chen K, Koboldt DC, Abbott TE, Dooling DJ, et al. SomaticSniper: identification of somatic point mutations in whole genome sequencing data. Bioinformatics. 2012 Feb 1; 28(3):311–7. [PubMed: 22155872]
41. McKenna A, Hanna M, Banks E, Sivachenko A, Cibulskis K, Kernytsky A, et al. The Genome Analysis Toolkit: a MapReduce framework for analyzing next-generation DNA sequencing data. Genome Res. 2010 Sep; 20(9):1297–303. [PubMed: 20644199]
42. Koboldt DC, Zhang Q, Larson DE, Shen D, McLellan MD, Lin L, et al. VarScan 2: somatic mutation and copy number alteration discovery in cancer by exome sequencing. Genome Res. 2012 Mar; 22(3):568–76. [PubMed: 22300766]
43. Walter MJ, Shen D, Ding L, Shao J, Koboldt DC, Chen K, et al. Clonal architecture of secondary acute myeloid leukemia. N Engl J Med. 2012 Mar 22; 366(12):1090–8. Epub 2012/03/16. eng. [PubMed: 22417201]
44. Ester, M.; Kriegel, HP.; Sander, J.; Xu, X. A density-based algorithm for discovering clusters in large spatial databases with noise. Proceedings of 2nd International Conference on Knowledge Discovery and Data Mining; 1996. p. 1232-9.
45. Fraley C, Raftery A. Model-based clustering, discriminant analysis and density estimation. Journal of American Statistical Association. 2002; 97:611–31.
46. Levine RL, Belisle C, Wadleigh M, Zahrieh D, Lee S, Chagnon P, et al. X-inactivation-based clonality analysis and quantitative JAK2V617F assessment reveal a strong association between clonality and JAK2V617F in PV but not ET/MMM, and identifies a subset of JAK2V617F-negative ET and MMM patients with clonal hematopoiesis. Blood. 2006 May 15; 107(10):4139–41. [PubMed: 16434490]
47. Ding L, Ley TJ, Larson DE, Miller CA, Koboldt DC, Welch JS, et al. Clonal evolution in relapsed acute myeloid leukaemia revealed by whole-genome sequencing. Nature. 2012 Jan 26; 481(7382): 506–10. Epub 2012/01/13. eng. [PubMed: 22237025]

48. Oh ST, Gotlib J. JAK2 V617F and beyond: role of genetics and aberrant signaling in the pathogenesis of myeloproliferative neoplasms. Expert Rev Hematol. 2010 Jun; 3(3):323–37. Epub 2010/11/19. eng. [PubMed: 21082983]

49. Zhang SJ, Rampal R, Manshouri T, Patel J, Mensah N, Kayserian A, et al. Genetic analysis of patients with leukemic transformation of myeloproliferative neoplasms shows recurrent SRSF2 mutations that are associated with adverse outcome. Blood. 2012 May 10; 119(19):4480–5. [PubMed: 22431577]

50. Steensma DP, Pardanani A, Stevenson WS, Hoyt R, Kiu H, Grigg AP, et al. More on Myb in myelofibrosis: molecular analyses of MYB and EP300 in 55 patients with myeloproliferative disorders. Blood. 2006 Feb 15; 107(4):1733–5. author reply 5. [PubMed: 16461764]

51. Ding Y, Harada Y, Imagawa J, Kimura A, Harada H. AML1/RUNX1 point mutation possibly promotes leukemic transformation in myeloproliferative neoplasms. Blood. 2009 Dec 10; 114(25): 5201–5. [PubMed: 19850737]

52. Dey A, Seshasayee D, Noubade R, French DM, Liu J, Chaurushiya MS, et al. Loss of the tumor suppressor BAP1 causes myeloid transformation. Science. 2012 Sep 21; 337(6101):1541–6. [PubMed: 22878500]

53. Abdel-Wahab O, Dey A. The ASXL-BAP1 axis: new factors in myelopoiesis, cancer and epigenetics. Leukemia. 2013 Jan; 27(1):10–5. [PubMed: 23147254]

54. Ruan HB, Han X, Li MD, Singh JP, Qian K, Azarhoush S, et al. O-GlcNAc transferase/host cell factor C1 complex regulates gluconeogenesis by modulating PGC-1alpha stability. Cell metabolism. 2012 Aug 8; 16(2):226–37. [PubMed: 22883232]

55. Godfrey AL, Chen E, Pagano F, Ortmann CA, Silber Y, Bellosillo B, et al. JAK2V617F homozygosity arises commonly and recurrently in PV and ET, but PV is characterized by expansion of a dominant homozygous subclone. Blood. 2012 Sep 27; 120(13):2704–7. [PubMed: 22898600]

56. Scott LM, Scott MA, Campbell PJ, Green AR. Progenitors homozygous for the V617F mutation occur in most patients with polycythemia vera, but not essential thrombocythemia. Blood. 2006 Oct 1; 108(7):2435–7. eng. [PubMed: 16772604]

57. Hou Y, Song L, Zhu P, Zhang B, Tao Y, Xu X, et al. Single-cell exome sequencing and monoclonal evolution of a JAK2-negative myeloproliferative neoplasm. Cell. 2012 Mar 2; 148(5): 873–85. [PubMed: 22385957]

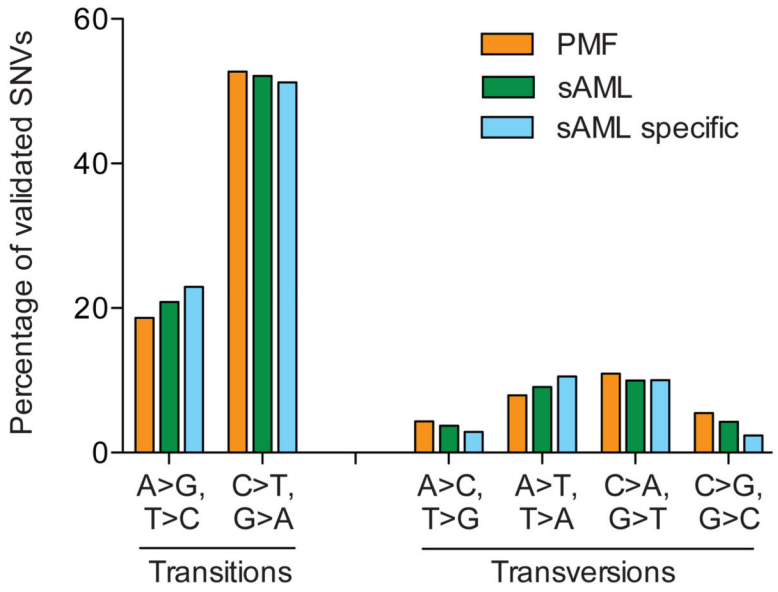

Figure 1. Spectrum of transition and transversion mutations per sample

The percentage of somatic single nucleotide variants (SNVs) in the PMF, sAML, or specific for the sAML sample are categorized by transition and transversion mutation types.

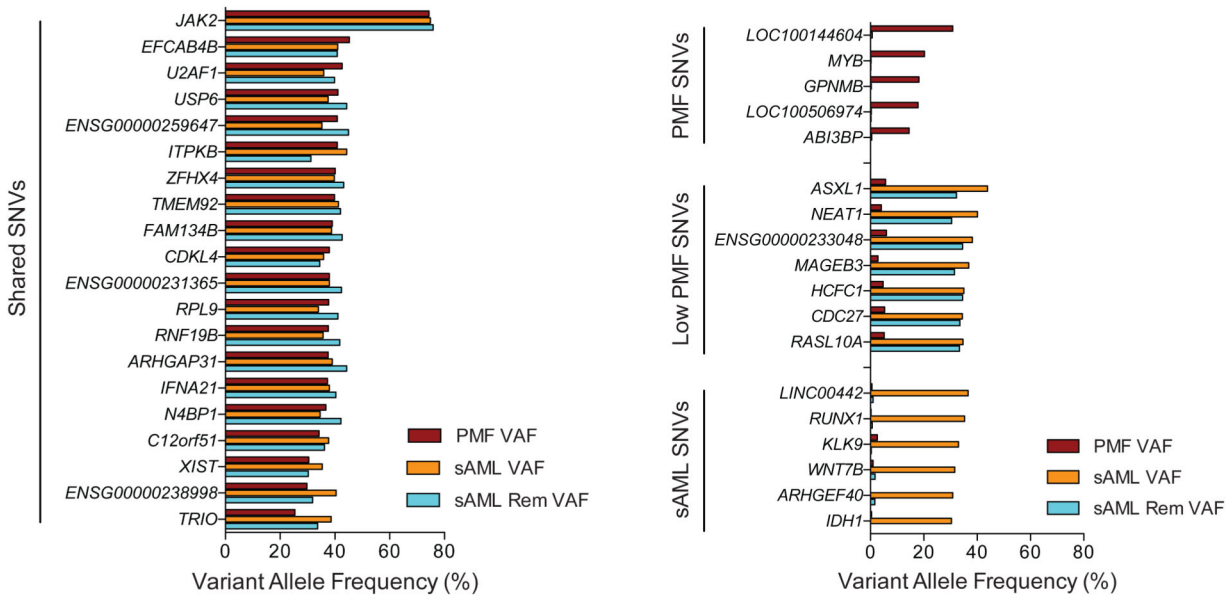

Figure 2. Comparison of variant allele frequencies across tier 1 somatic single nucleotide variants (SNVs)

The variant allele frequency for each tier 1 SNV across the PMF, sAML, and sAML remission/relapsed PMF samples is shown. The genes with the SNVs are divided based on whether the SNV was present predominantly in all three samples (Shared SNVs), only the PMF sample (PMF SNVs), low in the PMF sample but high in sAML and sAML remission/relapsed PMF samples (Low PMF SNVs), and only in the sAML sample (sAML SNVs).

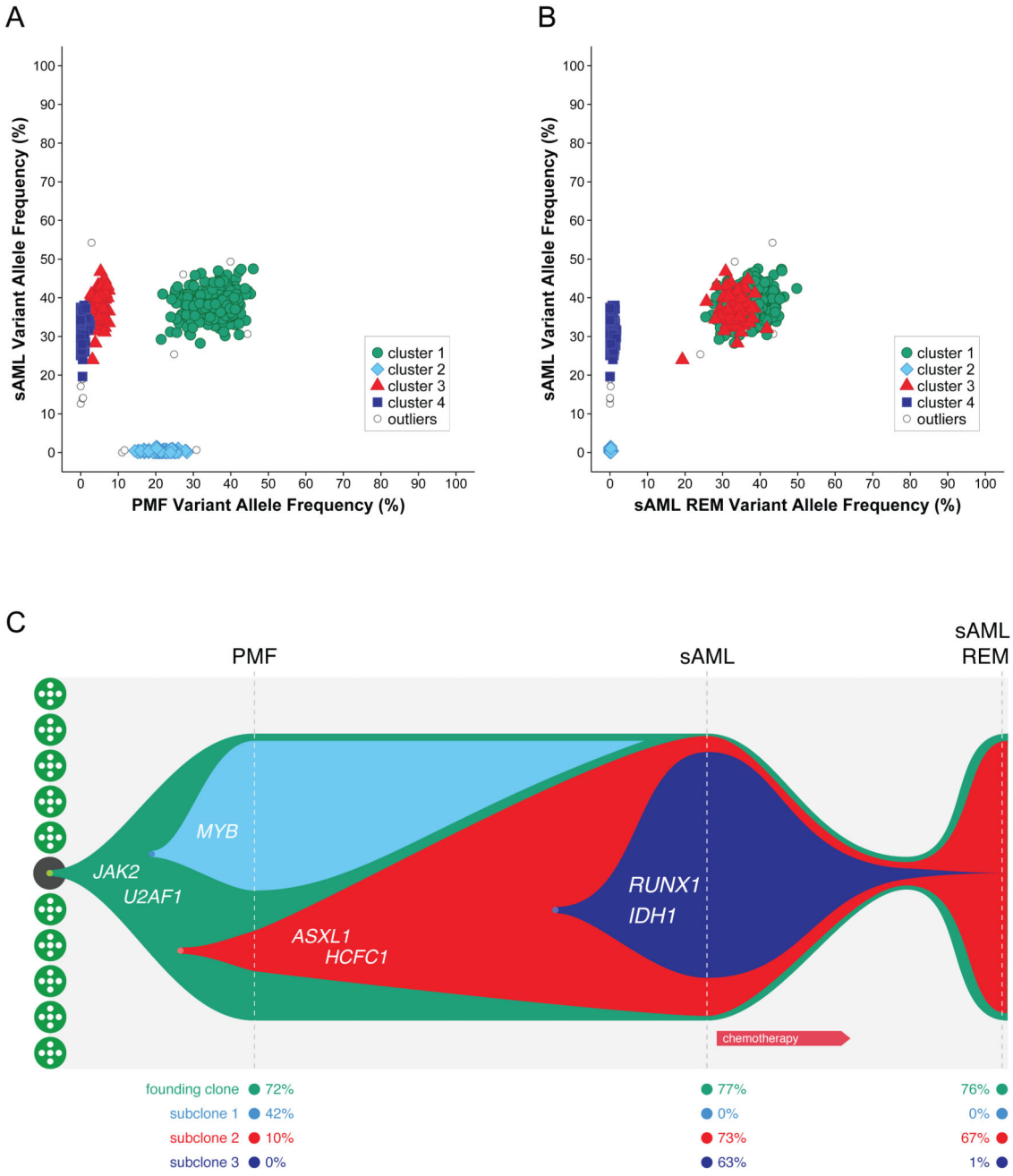

Figure 3. Clustering and clonal evolution across disease progression

Unsupervised clustering of 649 SNVs identified clusters of mutations with similar variant allele frequencies corresponding to the founding clone (green), subclone 1 (light blue), subclone 2 (red), and subclone 3 (dark blue). (A) Frequency of mutations in PMF versus sAML. (B) Frequency of mutations in sAML remission/relapsed PMF versus sAML. (C) A model of clonal evolution based on the median values for the VAFs in each of the four clusters at each stage of progression in (A) and (B) as shown below the plot. Abbreviations:

PMF, primary myelofibrosis; sAML, secondary acute myeloid leukemia; sAML REM, secondary acute myeloid leukemia remission/relapsed PMF.

Table 1

Somatic single nucleotide variant (SNV) mutations per tier

The number of SNV mutations validated for each sample per tier. sAML specific mutations are the mutations gained between the PMF sample and the sAML sample. Abbreviations: PMF, primary myelofibrosis; sAML, secondary acute myeloid leukemia.

	PMF	sAML	sAML specific	sAML Remission/Relapsed PMF[1]	Total
Tier 1	25	33	13	27	38
Tier 2	81	96	28	80	109
Tier 3	334	433	168	327	502
Overall	440	562	209	434	649

[1] Only includes SNVs identified in WGS sequencing of the PMF or sAML samples

Table 2

Putative driver somatic single nucleotide variants (SNVs) validated following whole genome sequencing

For each SNV, the normal gene function, effect of the mutation (if known), and the variant allele frequency (VAF) at each of the three disease stages is shown. Abbreviations: PMF, primary myelofibrosis; sAML, secondary acute myeloid leukemia.

Gene	Mutation	Normal Function/Effect of Mutation	PMF VAF	sAML VAF	sAML Remission/Relapsed PMF VAF
JAK2	V617F	Tyrosine kinase, hyperactivated JAK-STAT signaling	74.4%	74.9%	75.9%
U2AF1	Q157P	Splicing factor, possibly altered splicing	42.7%	36.0%	39.9%
MYB	E306K	Transcription factor, essential regulator of hematopoiesis	20.2%	0.2%	0.1%
ASXL1	Q692*	Transcriptional regulator, member of PRC2 complex, binds BAP1	5.7%	43.9%	32.3%
HCFC1	S2025Y	Transcriptional regulator, regulated by BAP1	4.7%	35.0%	34.5%
IDH1	R132C	Aberrant 2-HG production, altered DNA methylation	0.3%	30.3%	0.0%
RUNX1	D198N	Transcription factor, CBF subunit	0.2%	35.3%	0.7%

Table 3

***JAK2* V617F and *U2AF1* Q157P genotypes from cultured CD34+ cell derived colonies**

Colonies were isolated from the peripheral blood at the PMF stage and were genotyped for *JAK2* V617F and *U2AF1* Q157P mutations. The number of colonies with each genotype is shown. Abbreviations: WT, Het, and Hom correspond to colonies that are wildtype, heterozygous, or homozygous for the mutation, respectively. PMF, primary myelofibrosis.

	***JAK2* WT**	***JAK2* Het**	***JAK2* Hom**	**Total colonies**
U2AF1 WT	11	1	1	13 (31%)
U2AF1 Het	0	1	28	29 (69%)
U2AF1 Hom	0	0	0	0 (0%)
Total colonies	11 (26%)	2 (5%)	29 (69%)	42